ELSEVIER

Journal of Fluids and Structures 26 (2010) 430–441

JOURNAL OF FLUIDS AND STRUCTURES

www.elsevier.com/locate/jfs

A modified wake oscillator model for vortex-induced vibration of circular cylinders for a wide range of mass-damping ratio

A. Farshidianfar*, H. Zanganeh

Department of Mechanical Engineering, Faculty of Engineering, Ferdowsi University of Mashhad, PO Box 91775-1111, Mashhad, Iran

Received 1 December 2008; accepted 6 November 2009
Available online 12 March 2010

Abstract

In this paper, the behavior of an elastically mounted cylinder, subjected to vortex-induced vibrations (VIV), is investigated by a low-dimensional model. The classical wake oscillator model, as a standard model, predicts the behavior of the system at high mass-damping ratios but fails in modeling the system at low mass-damping ratios. A modified wake oscillator model is introduced in order to describe the response of the system over a wide range of mass-damping ratios. The results of this new model are compared to experimental results from the literature and shown to be in good agreement. The new model can describe most of the features of vortex-induced vibration phenomenology, such as the Griffin plot and lock-in domains.

Keywords: VIV; Wake oscillator model; van der Pol equation; Griffin plot

1. Introduction

The highly specialized subject of vortex-induced vibrations (VIVs) is part of a number of disciplines, incorporating fluid mechanics, structural mechanics, vibrations, computational fluid dynamics (CFD), acoustics, wavelet transforms, complex demodulation analysis, statistics, and smart materials. They occur in many engineering situations, such as bridges, stacks, transmission lines, aircraft control surfaces, offshore structures, thermowells, engines, heat exchangers, marine cables, towed cables, drilling and production risers in petroleum production, mooring cables, moored structures, tethered structures, buoyancy and spar hulls, pipelines, cable-laying, members of jacketed structures, and other hydrodynamic and hydroacoustic applications (Sarpkaya, 2004). The practical significance of VIV has led to a large number of fundamental studies, many of which are discussed in the comprehensive reviews of Parkinson (1989), Sarpkaya (2004), and Williamson and Govardhan (2007).

The VIV phenomenon is result of the interaction between fluid and structure. A cross-flow flowing past bluff bodies is usually unsteady. Beyond a critical Reynolds number, the boundary layer will separate from each side of the body to form the so-called Kármán vortex street. The alternately shed vortices from the body generate periodic forces on the structure, causing a structural vibration. The structural motion in turn influences the flow field, giving rise to nonlinear fluid–structure interaction. As the flow velocity is increased or decreased so that the shedding frequency approaches the natural frequency of the structure, the vortex shedding frequency suddenly locks onto the structural natural frequency.

*Corresponding author. Tel.: +98 511 8781151; fax: +98 511 6078632.
E-mail address: farshid@um.ac.ir (A. Farshidianfar).

0889-9746/$ - see front matter © 2010 Elsevier Ltd. All rights reserved.
doi:10.1016/j.jfluidstructs.2009.11.005

The resultant vibrations occur at or nearly at the natural frequency of the structure and vortices in the near wake input energy to the cylinder. Large amplitude vortex-induced structural vibration can result (Blevins, 1990).

As was mentioned above, during lock-in, the frequency of vortex-shedding synchronizes with the natural frequency of the structure. However, this synchronization does not occur in the same manner at high and low values of mass-damping ratio. For high mass ratios, these two frequencies become equal within the lock-in regime (Feng, 1968). On the other hand for low mass ratios the body oscillates at a distinctly higher frequency (Khalak and Williamson, 1997).

The maximum structural displacement at lock-in is expressed as a function of combined mass-damping parameter, the so-called Skop–Griffin parameter S_G (Skop, 1974). Skop and Griffin compiled several different experimental data to predict response amplitudes. The results of compilations of many different investigations were plotted in a log–log form by Griffin (1980). This plot is called the Griffin plot and is extensively used by practicing engineers (Khalak and Williamson, 1999).

Different semi-empirical models have been used for describing VIV and lock-in phenomena, including wake oscillator models (Bishop and Hassan, 1963; Hartlen and Currie, 1970; Griffin et al., 1973; Skop and Griffin, 1973), SDOF models that use a single ordinary differential equation to describe the behavior of structural oscillator (Basu and Vickery, 1983; Simiu and Scanlan, 1986; Goswami et al., 1993), force decomposition models in which the lift force is decomposed into a fluid inertia force related to structure displacement and a fluid damping force related to structure velocity (Griffin, 1980; Griffin and Koopman, 1997), and variational approaches (McIver, 1973; Benaroya and Wei, 2000).

The coupling of fluctuating lift force and vibrating structure can be modeled by a simple wake oscillator model. In such models, the wake dynamics is assumed to follow a van der Pol equation. In fact, it is sufficient to have a self-sustained oscillator with a limit cycle. The bluff body is then modeled by another oscillator excited by the wake variable (de Langre, 2006). The effect of the motion of the structure on the wake is represented by a forcing term in the van der Pol equation that can be proportional to displacement, velocity or acceleration of bluff body. Facchinetti et al. (2004) have shown that the most appropriate forcing term is proportional to the acceleration of the bluff body.

The classical wake oscillator model fails to predict the variation in the behavior of the system at low values of the mass-damping ratio. Therefore, a modified wake oscillator model is introduced. Its analysis shows that the modified model is considerably more accurate than the classical model and can be used over a wide range of mass-damping ratios.

2. Classical wake oscillator model

Due to their occurrence in various scientific fields, ranging from biology, chemistry, physics to engineering, coupled nonlinear oscillators have been a subject of particular interest in recent years (Rand and Holmes, 1980; Woafo et al., 2005). Among these coupled systems, a particular class is the fluid–structure interaction system, which can be modeled by phenomenological models based on wake oscillators. These models explain and simulate experimental results and thus help understanding the physics of VIV, especially when computational limits arise for flow-field numerical simulations. Therefore, in this section the classical wake oscillator model, commonly used in the literature (Facchinetti et al., 2004; de Langre, 2006), is analyzed.

2.1. VIV model

The structure is an elastically mounted cylinder of diameter D. It is subjected to the fluid flow of steady velocity U and can oscillate transversely to fluid flow, Fig. 1. The motion of this cylinder can be modeled by a simple linear equation that is affected by fluid loading

$$(m_s + m_f)\ddot{Y} + (c_s + c_f)\dot{Y} + kY = S, \tag{1}$$

where overdots mean derivatives with respect to dimensional time T, and Y is the in-plane displacement of cylinder, transversely to fluid flow, m_s and k are, respectively, the mass and the stiffness of the cylinder in absence of fluid, c_s models viscous dissipation in supports, m_f is fluid-added mass, which models inviscid inertia effects of fluid (Blevins, 1990), and c_f the fluid-added damping, and read

$$m_f = \frac{1}{4}\pi C_m \rho D^2, \quad c_f = \frac{2\pi \mathrm{St} U}{D}\gamma \rho D^2, \tag{2}$$

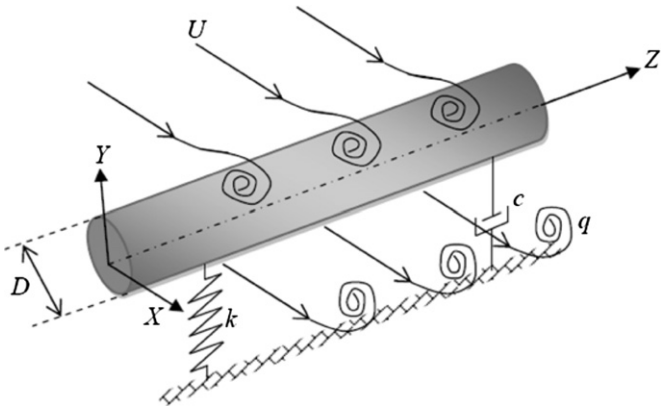

Fig. 1. Model of elastically mounted cylinder coupled with wake oscillators for 2-D vortex-induced vibrations.

where ρ is the fluid density, $C_m=1$ the added mass coefficient for a circular cylinder (Blevins, 1990), St the Strouhal number, and γ the fluid added damping coefficient depending on the mean sectional drag coefficient C_D (Blevins, 1990). We assume that $\gamma=0.8$ (Facchinetti et al., 2004).

The forcing term S models the effects of vortices on structure and is defined as

$$S=\frac{1}{2}\rho U^2 D C_L, \tag{3}$$

where C_L is the fluctuating lift coefficient.

The fluctuating nature of the vortex street can be modeled by a van der Pol oscillator (Nayfeh, 1993)

$$\ddot{q}+\varepsilon_f\Omega(q^2-1)\dot{q}+\Omega_f^2 q=\frac{A}{D}\ddot{Y}, \tag{4}$$

where $\Omega_f=2\pi U\mathrm{St}/D$ is the vortex-shedding frequency, ε and A are the parameters that can be derived from experimental results. Facchinetti et al. (2004) found that $\varepsilon=0.3$ and $A=12$. q is the dimensionless wake variable defined by $q(t)=2C_L(t)/C_{L0}$, where C_{L0} is the reference lift coefficient of a stationary cylinder subjected to vortex shedding and is usually taken as $C_{L0}=0.3$ (Blevins, 1990; Pantazopoulos, 1994).

Eqs. (1) and (4) lead to the coupled fluid-structure dynamical system. There are different coupling methods, such as displacement coupling (Krenk and Nielsen, 1999), velocity coupling (Mureithi et al., 2000; Plaschko, 2000), and acceleration coupling (Blevins, 1990; Parkinson, 1989). Facchinetti et al. (2004) have shown that the most appropriate coupling is the acceleration coupling. So, in this first section, for the classical model, an acceleration coupling is used.

Eqs. (1) and (4) can be put in a dimensionless form by introducing the dimensionless terms of $t=(k/m)^{1/2}T$ and $y=Y/D$ (de Langre, 2006)

$$\begin{cases} \ddot{y}+\lambda\dot{y}+y=M\Omega^2 q, \\ \ddot{q}+\varepsilon\Omega(q^2-1)\dot{q}+\Omega^2 q=A\ddot{y}, \end{cases} \tag{5}$$

where $\Omega=\mathrm{St}U_r$ is the dimensionless frequency of a self-sustained oscillation of the wake (de Langre, 2006), $U_r=U/f_v D$ the reduced velocity, and f_v the vortex-shedding frequency. λ is the damping coefficient and M is a mass number, which scales the effects of the wake on the structure (Facchinetti et al., 2004). They are given by

$$\lambda=2\xi+\frac{\gamma}{\mu}\Omega, \quad M=\frac{C_{L0}/2}{8\pi^2\mathrm{St}\mu}, \quad \mu=\frac{m_s+m_f}{\rho D^2}, \tag{6}$$

where ξ is the structure-reduced damping, $\xi=c_s/2\sqrt{mk}$.

3. Modified wake oscillator model

The classical wake oscillator model, described in the previous sections, is able to capture the behavior of the system at high mass-damping ratios (Facchinetti et al., 2004) but, as will be shown, cannot predict its behavior at low mass-damping ratios. In this section a modified wake oscillator model able to predict the behavior of the system at both low and high mass-damping ratios will be presented.

3.1. VIV model

It is believed that a model trying to accurately predict VIV must be able to describe the oscillations in which small oscillations feed energy into the system and large oscillations remove it (Klamo, 2007). Also VIV is an inherently nonlinear and self-regulated phenomenon (Sarpkaya, 2004). These characteristics must be considered in every VIV model.

In other engineering fields, such as electrical engineering (Lynch, 1995), biological and chemical structures (Mirollo and Strogatz, 1990), and laser dynamics (Wirkus and Rand, 2002), systems with similar characteristics can be found, for example, interaction of microwave oscillators in the case of electrical engineering. Two important characteristics of these oscillators are negative resistance (which causes the amplitude of the oscillations to grow) and gain saturation (which limits the amplitude of the oscillation) (Maas, 1988). In such systems the interaction of oscillators is modeled by two coupled van der Pol equations (Wirkus, 1999).

These observations can guide one to use two coupled van der Pol equations to model the VIV phenomenon, too. It means that not only the wake dynamics but also the structural oscillations can be modeled by a van der Pol equation. The description of the structural oscillations by a van der Pol equation was used in the work of Teufel et al. (2006). They modeled two aerodynamically excited pendula by two coupled van der Pol equations. Although their model was not a wake oscillator model, it showed the possibility of using a van der Pol equation for structural oscillations.

As mentioned in previous sections, two equations of the system can be coupled via three different coupling terms, including acceleration, velocity, and displacement coupling. While for the classical wake oscillator model, Facchinetti et al. (2004) showed that the acceleration coupling works better than the other ones, in the present work, the selection of coupling term is based on the comparison of the results of all three distinct coupling terms.

According to these assumptions, the equations of the system can be expressed as

$$\begin{cases} \ddot{y} + \varepsilon\lambda(y^2-1)\dot{y} + y = M\Omega^2 q, \\ \ddot{q} + \varepsilon\Omega(q^2-1)\dot{q} + \Omega^2 q = F, \end{cases} \tag{7}$$

where F can be $A\dot{y}$, $A\ddot{y}$, or Ay for velocity, acceleration, and displacement coupling, respectively. The values of ε and A are obtained by comparing the experimental data with the results of the new model.

3.2. Lift magnification factor

It is generally accepted that cylinder motion has an effect on the lift force. Experimental data demonstrates that lift increases with response amplitude up to a point, then decreases with further increase in amplitude (Pantazopoulos, 1994). In this section, using the modified wake oscillator model, the relation between lift force and the response amplitude is derived.

Using a harmonic linearization method for Eq. (7) and assuming $y = y_0 e^{i\omega t}$ and $q = q_0 e^{i(\omega t+\varphi)}$ and defining a reference lock-in state by $\omega = 1$ and $\Omega = 1$, elementary algebra yields

$$q_0^4 - 4q_0^2 - 4\frac{\lambda}{M}Ay_0^2\left(\frac{y_0^2}{4}-1\right) = 0. \tag{8}$$

Considering the real roots of Eq. (8), the vortex lift magnification factor with respect to a stationary structure experiencing vortex shedding, $K = q_0/2$, is derived as

$$K = \frac{1}{2}\sqrt{2 + 2\sqrt{1 - \frac{\lambda}{M}Ay_0^2\left(\frac{y_0^2}{4}-1\right)}}. \tag{9}$$

This equation shows the relation between the lift magnification factor and the amplitude of the structural oscillations. Assuming $S_G = 1$, Fig. 2 shows the effect of the value of the coupling parameter A on the system by matching the model response, Eq. (9), to experimental data on the lift magnification factor. Facchinetti et al. (2004), in the same calculations for the classical model, proposed the value of $A = 12$. Referring to their results, Fig. 2 shows that the results of the modified wake oscillator model at $A = 12$ are quite consistent with their results at $A = 12$. Therefore, the value of $A = 12$ is proposed for the modified wake oscillator model, too.

As mentioned before, experiments show that the lift magnification increases with response amplitude up to a point and then becomes a decreasing function of y_0 (Pantazopoulos, 1994). Facchinetti et al. (2004) showed that the classical

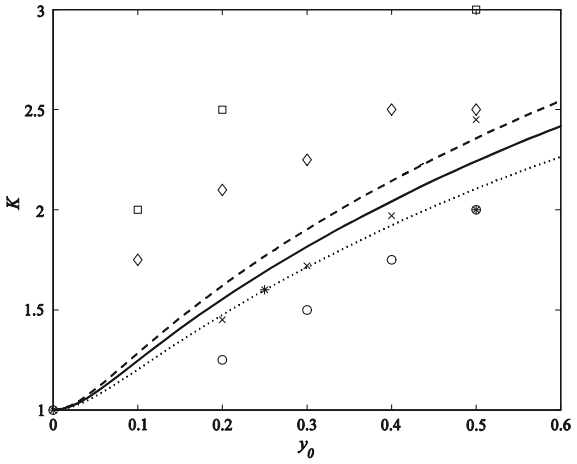

Fig. 2. Lift magnification K as a function of the imposed structure motion amplitude y_0 which is compared to experimental data: ◇, Vickery and Watkins (1962); ×, Bishop and Hassan (1964); *, King (1977); □, Griffin (1980); ○, Pantazopoulos (1994). Model parameters: …, $A=9$; —, $A=12$ (proposed value); - - -, $A=15$.

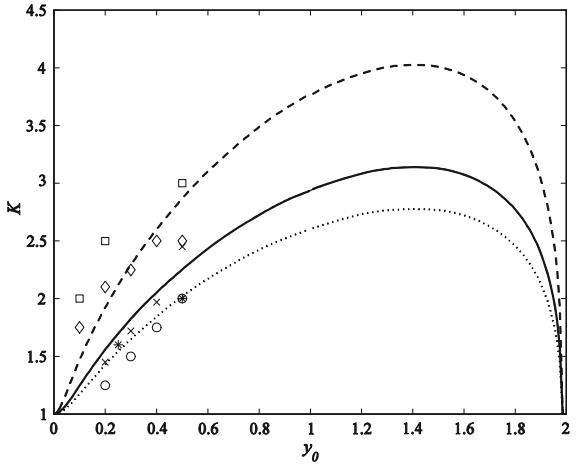

Fig. 3. Lift magnification K as a function of the imposed structure motion amplitude y_0 in low and high mass-damping ratios and the experimental results of: ◇, Vickery and Watkins (1962); ×, Bishop and Hassan (1964); *, King (1977); □, Griffin (1980); ○, Pantazopoulos (1994). …, $S_G=0.1$; —, $S_G=1$; - - -, $S_G=5$.

wake oscillator model cannot predict this feature. Also, parameters other than structure oscillation amplitude and frequency, on which that the lift magnification might depend, were not considered in their approach. But, as can be seen from Eq. (9), in the new model, in addition to the structure oscillation amplitude and frequency, the effect of mass and damping parameters is considered. Fig. 3 shows the lift magnification for different values of the mass mass-damping ratio.

The experimental results of Fig. 3 vary from experiments that were conducted at low mass-damping ratios (Bishop and Hassan, 1964), to the experiments that were conducted at high mass-damping ratios (Griffin, 1980). These experimental results illustrate that higher mass-damping ratios cause higher lift magnification factor. Fig. 3 indicates that the modified wake oscillator model can predict this feature. Also it shows that, first, the lift magnification increases with respect to y_0 and then becomes a decreasing function of y_0, which is similar to the experimental data. Therefore, the modified wake oscillator model can predict the behavior of the system for both low and high mass-damping.

3.3. Maximum amplitude at lock-in

The maximum structure displacement amplitude at lock-in can be expressed as a function of a single combined mass-damping parameter, namely the Skop–Griffin parameter S_G (Facchinetti et al., 2004)

$$S_G = 8\pi^2 \mathrm{St}\mu\xi = \frac{C_{L0}\xi}{2M}, \tag{10}$$

yielding the so-called Griffin plot. The major task of this section, using the modified wake oscillator model, is to provide a better approximation of the structure displacement amplitude at lock-in over much of the S_G range.

Using a harmonic linearization method for Eq. (7) and assuming $y = y_0 e^{i\omega t}$ and $q = q_0 e^{i(\omega t+\varphi)}$ and assuming $\varphi = \pi/4$ and defining a reference lock-in state by $\omega = 1$ and $\Omega = 1$, as done by Facchinetti et al. (2004) for the classical model, Eq. (7) yields

$$B^4 - 3B^3 + 3B^2 - \left(\frac{1}{\varepsilon^2}\frac{M^2}{\lambda^2} + 1\right)B + \frac{1}{\varepsilon^2}\frac{M^2}{\lambda^2} - \frac{A}{\varepsilon^4}\frac{M^3}{\lambda^3} = 0, \tag{11}$$

where $B = y_0^2/4$. Using Eqs. (6) and (10) and assuming $M = 0.05/\mu$, M/λ can be written in terms of the S_G parameter

$$\frac{\lambda}{M} = \frac{4S_G}{C_{L0}} + 20\gamma\Omega; \tag{12}$$

hence,

$$y_0 = 2\sqrt{|B|}. \tag{13}$$

Also, using the same process, the classical model yields

$$y_0 = 2\left(\frac{M}{\lambda}\right)\sqrt{1 + \left(\frac{A}{\varepsilon}\right)\left(\frac{M}{\lambda}\right)}, \tag{14}$$

which is the reproduction of the result obtained by Facchinetti et al. (2004).

Fig. 4 presents the results of Eqs. (11) and (13) for three different values of ε and the result of the classical model, which are compared with the experimental data of the Griffin plot. While for all values of ε the modified model qualitatively predicts the Griffin plot, it is only for $\varepsilon = 0.3$ that the results are qualitatively consistent with the experimental data. Therefore, the value of $\varepsilon = 0.3$ is proposed for the modified wake oscillator model, which is the same as the value proposed by Facchinetti et al. (2004) for the classical model. The similarity of the values of these parameters in the classical and modified models allows a comparison between these two models. Also, Fig. 4 clearly shows that the results of the modified wake oscillator model are considerably more accurate than the classical model

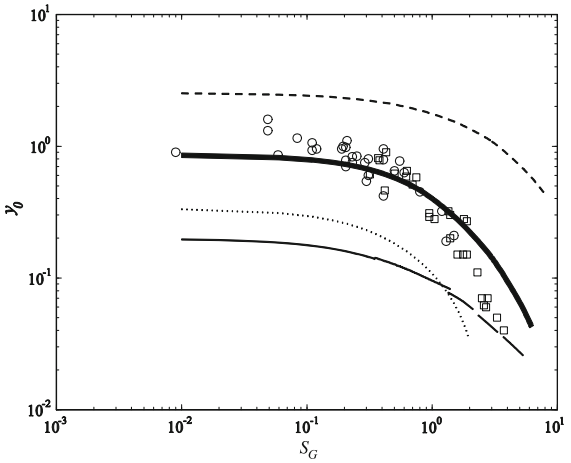

Fig. 4. Structural oscillation amplitude at lock-in as a function of S_G. —, Classical wake oscillator model. Results of the modified wake oscillator model: - - -, $\varepsilon = 0.1$; ▬, $\varepsilon = 0.3$; …, $\varepsilon = 0.5$. Empirical data in water: ○, Skop and Balasubramanian (1997). Empirical data in air: □, Skop and Balasubramanian (1997).

ones. It also illustrates that the modified model can, both qualitatively and quantitatively, predict the collapse of amplitude in the Griffin plot.

3.4. Frequency response

In previous sections, the particular choice of coupling terms did not affect the results, because the reference state was defined as $\omega=1$. When the frequency response is sought, however, a coupling model must be considered. In this section, the frequency response of the modified model is obtained.

Using a process similar to that used by Facchinetti et al. (2004) for the classical model, the equation of the angular frequency will be

$$-\omega^6+(\Omega^2-p^2+2)\omega^4+AM\Omega^2\omega^3+(\Omega^2(p^2-2)-1)\omega^2-AM\Omega^2\omega+\Omega^2=0, \tag{15}$$

$$-\omega^6+(\Omega^2-p^2+2+AM\Omega^2)\omega^4+(\Omega^2(p^2-AM-2)-1)\omega^2+\Omega^2=0, \tag{16}$$

$$-\omega^6+(\Omega^2-p^2+2)\omega^4+(\Omega^2(p^2-2+AM)-1)\omega^2+(1-AM)\Omega^2=0, \tag{17}$$

which are for velocity, acceleration, and displacement coupling, respectively, and p is $\varepsilon\lambda(\frac{1}{4}y_0^2-1)$. The value of y_0 is dependent on the value of Ω. So, for each Ω the value of y_0 is evaluated by solving Eq. (7) numerically, via a fourth order Runge–Kutta method with an initial condition of $q(0)=2$.

Also, using the same process, the classical model yields

$$-\omega^6+(2-\lambda^2+\Omega^2(1+AM))\omega^4+(\Omega^2(\lambda^2-AM-2)-1)\omega^2+\Omega^2=0. \tag{18}$$

Figs. 5 and 6 show the comparison of the frequency response of the classical and modified wake oscillator model, respectively, for the case of low mass-damping ratios, with experimental results of Branković and Bearman (2006) for $m^*=0.82$ and $\xi=1.5\times10^{-4}$. The mass ratio m^* is defined as

$$m^*=\frac{4m_s}{\pi\rho D^2 l}, \tag{19}$$

where l is the length of the cylinder, which in the case of Branković and Bearman (2006) is $l=584$ mm. Combining Eqs. (2), (6) and (19) yields

$$m^*l=\frac{4}{\pi}\mu-C_m. \tag{20}$$

This experimental data illustrates that during lock-in, the frequency departs from unity and this behavior differs considerably from what is seen in experiments in high mass-damping ratios. This departure has previously been

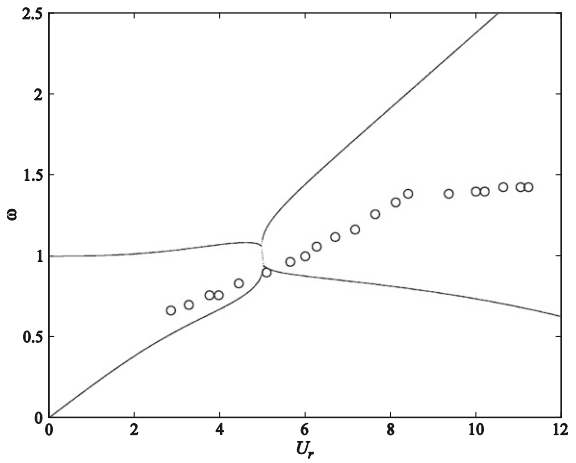

Fig. 5. Frequency response of the classical model for low mass-damping ratio ($\mu=1.1615$, $\xi=1.5\times10^{-4}$). —, The classical wake oscillator model; ○, Branković and Bearman's experimental results (2006).

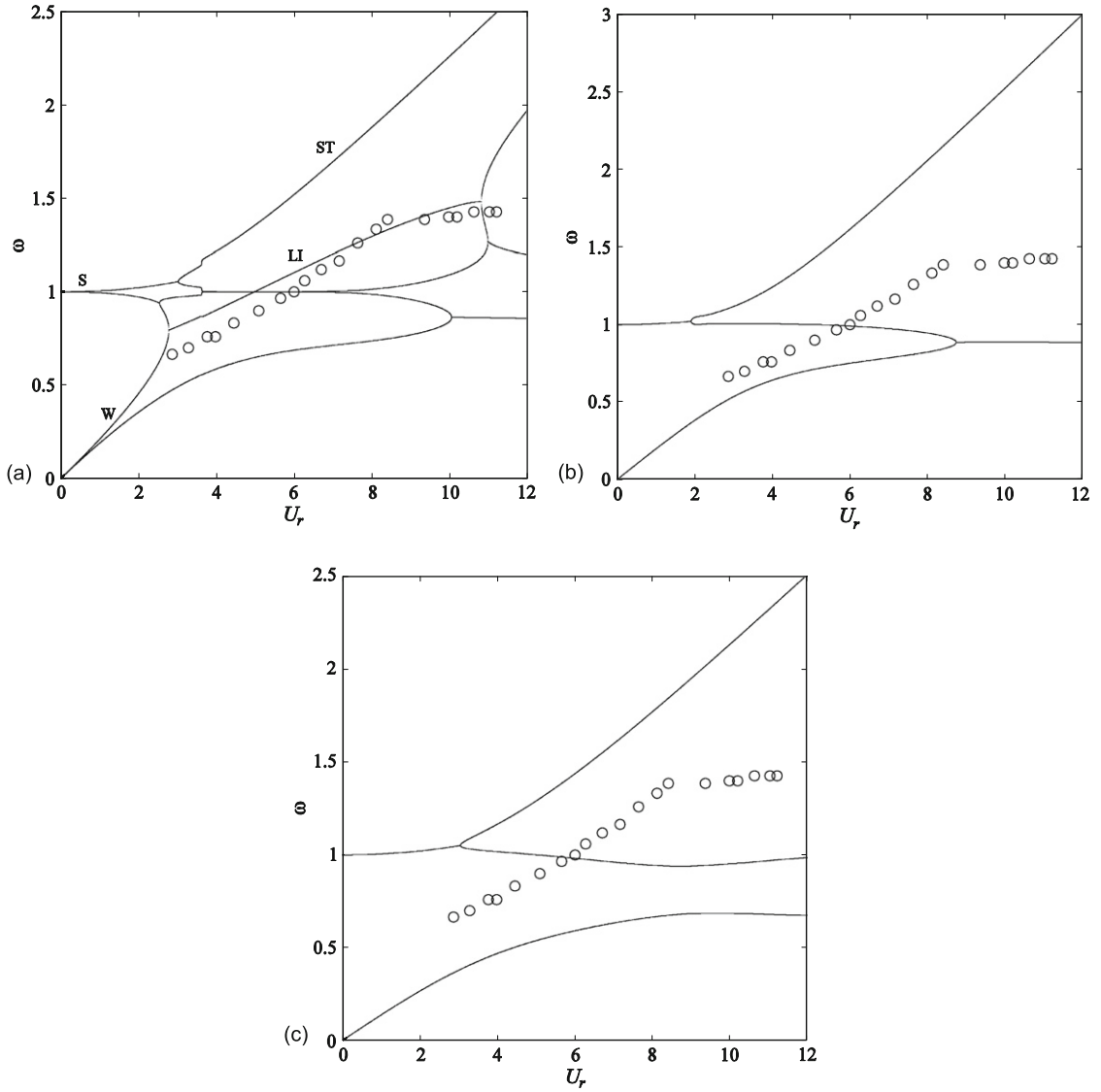

Fig. 6. Frequency respose of the modified model at low values of the mass-damping ratio for three different coupling terms: —, modified model with (a) velocity coupling, (b) acceleration coupling, (c) displacement coupling; ○, experimental data of Branković and Bearman (2006) for $m^*=0.82$, $l=0.584$ m and $\xi=1.5\times10^{-4}$ ($\mu=1.1615$); St, Strouhal law branch; W, wake; S, structure; LI, lock-in.

demonstrated experimentally in recent work (Moe and Wu, 1990; Khalak and Williamson, 1997, 1999; Gharib et al, 1998). This new behavior, as Khalak and Williamson (1997) believe, is the result of imposing a low mass-damping ratio. As seen, the classical model fails in predicting the behavior of the system in low mass ratio and just the modified wake oscillator model with velocity coupling can predict this new behavior and shows that the modified model again has a good agreement with the experimental results. Also Fig. 6 illustrates that, while for the classical model Facchinetti et al. (2004) have shown that the acceleraton coupling term works better than the other ones, velocity coupling is chosen for the modified model.

Fig. 7 shows the frequency response of the modified model for another low mass-damping ratio. It shows that the modified model has a good agreement with the experiment results.

Other branches of frequency response can occur under different conditions. For example, Fig. 8 shows the comparison of frequency response of the modified model and experimental results from a straked cylinder with $m^*=0.83$, $l=0.584$ m, and $\xi=2.5\times10^{-4}$. The strakes are 3-start with a pitch of five diameters and a height equal to 10% of the bare cylinder diameter. To model this cylinder, the mass ratio is defined as the effective mass of the

cylinder-displaced mass of water. Also, the reduced velocity U_r is calculated based on the diameter of the bare cylinder (Branković and Bearman, 2006).

Fig. 9 shows the frequency response of the modified model at high values of the mass-damping ratio and Feng's experimental results (1968) for comparison. As seen, the new model can also precisely predict the behavior of the system for high mass-damping ratios.

In recent figures all branches of the frequency response are shown. One of these branches corresponds to the Strouhal law, which is marked as ST in Fig. 6(a). As mentioned before, during lock-in, the frequency of vortex-shedding synchronizes with the natural frequency of the structure marked as W and S, respectively in Fig. 6(a). For high mass-damping ratios, these two branches lock onto each other in a constant value near unity. But, if the new branch, marked as LI in Fig. 6(a), tends to a value between the Strouhal law branch, ST, and unity, it is seen that lock-in will happen in other frequencies, as happens for low mass-damping ratios.

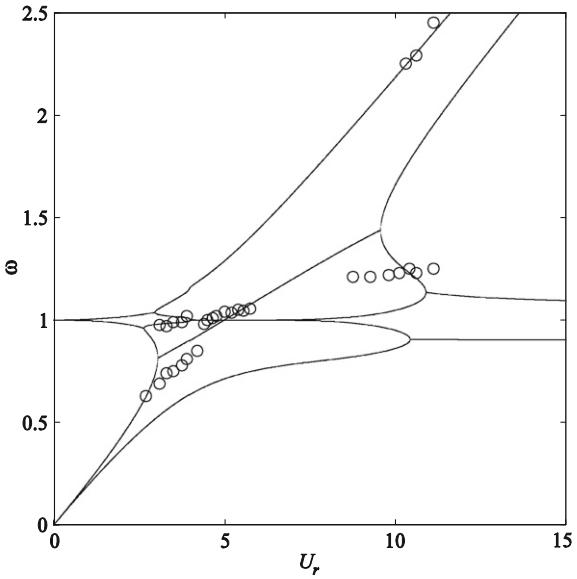

Fig. 7. Frequency respose of the modified model for low mass-damping ratio: —, modified model; ○, experimental data of Khalak and Williamson (1999) for $m^*=3.3$, $l=0.381$ m and $\xi=0.0026$ ($\mu=1.773$).

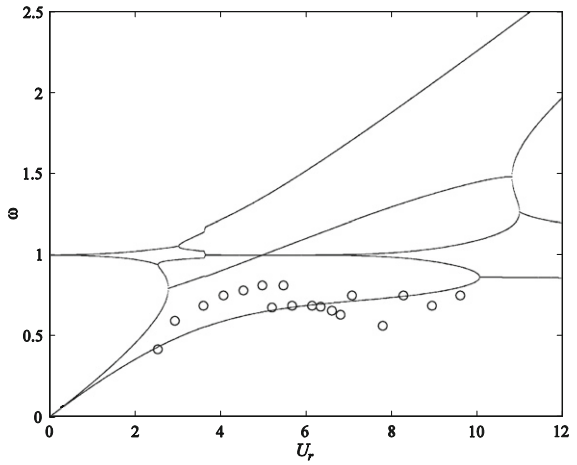

Fig. 8. Frequency respose of the modified model for low mass-damping ratio: —, modified model; ○, experimental data of Branković and Bearman (2006) for $m^*=0.83$, $l=0.584$ m and $\xi=2.5\times10^{-4}$ ($\mu=1.1661$).

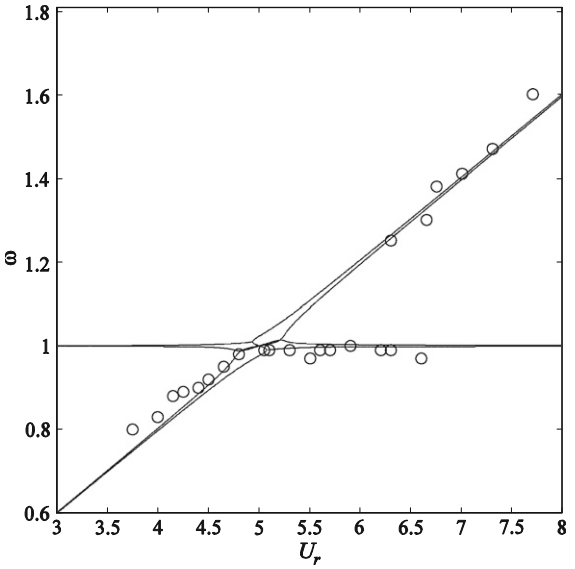

Fig. 9. Frequency respose of the modified model for high mass-damping ratio: —, modified model; ○, experimental data of Feng (1968) ($\mu = 194.55$ and $\lambda = 0.1$ (de Langre, 2006)).

4. Conclusions

Vortex-induced vibration (VIV) can severely limit the operation of structures and may even lead to catastrophic failure. The behavior of structures during VIV is different for low and high values of the mass-damping ratio. The comparison of the analysis of the classical wake oscillator model with empirical results showed that the classical wake oscillator model can only predict the behavior of the system at high mass-damping ratios. The failure of the classical wake oscillator model at low mass-damping ratios implies the need for a modified model. A modified wake oscillator has been presented here. In this new model, both structure and wake oscillator were modeled by van der Pol oscillators, which were coupled via a velocity coupling term. The selection of a velocity coupling term (recall that in the case of the classical model an acceleration coupling is used) is based on its superior results. A parameter study of the modified model shows that its parameters, A and ε, have the same values as in the classical model. This similarity allows a better comparison between two models.

It must be noted that although the new model can predict the behavior of the system for different flow velocities and for both low and high mass-damping ratios, it predicts self-oscillations for the cylinder at zero flow velocity, $\Omega = 0$, which is not physical.

Analysis of the frequency response, lift magnification factor, and the Griffin plot of this model, along with a comparison with both experimental results from the literature and the classical model, showed that the modified model describes the behavior seen at both high and low values of mass-damping ratio. Therefore, the new model can be applied over a wider range of applications from bridges and tall buildings to offshore structures.

Appendix. Harmonic linearization method

This method can be used to analyze both weakly and strongly nonlinear problems. By solving a simple nonlinear problem, this method is illustrated below. Consider the Duffing equation as follows:

$$\ddot{x} + x = \varepsilon x^3, \quad \dot{x}(0) = 0 \tag{21}$$

Physical insight leads us to the response $x = A\cos\omega t$ that satisfies the initial condition. Therefore,

$$x - \varepsilon x^3 = A\cos\omega t - \varepsilon A^3\cos^3\omega t = A\cos\omega t - \frac{\varepsilon A^3}{4}(3\cos\omega t + \cos 3\omega t), = A\cos\omega t\left[1 - \frac{3\varepsilon A^3}{4}\right] - \frac{\varepsilon A^3}{4}\cos 3\omega t, \tag{22}$$

Neglecting the third harmonic terms give

$$x-\varepsilon x^3 = A\cos\omega t\left[1-\frac{3\varepsilon A^3}{4}\right] = x\left[1-\frac{3\varepsilon A^3}{4}\right], \tag{23}$$

so that the Eq. (21) becomes

$$\ddot{x} + \left[1-\frac{3\varepsilon A^3}{4}\right]x = 0. \tag{24}$$

Therefore by assuming the response of the system as $x = A\cos\omega t$ we shall have

$$\omega^2 = 1-\frac{3\varepsilon A^3}{4}, \quad \omega \approx 1-\frac{3\varepsilon A^3}{8}, \quad x = A\cos\left[1-\frac{3\varepsilon A^3}{8}\right]t. \tag{25}$$

This result is the same as the response obtained by other methods, such as the method of Poincaré and Lindstedt or the Krylov and Bogoliubov method.

References

Basu, R.I., Vickery, B.J., 1983. Across-wind vibrations of structures of circular cross-section—part 2: development of a mathematical model for full-scale application. Journal of Wind Engineering and Industrial Aerodynamics 12, 75–97.

Benaroya, H., Wei, T., 2000. Hamilton's principle for external viscous fluid–structure interaction. Journal of Sound and Vibration 238, 113–145.

Bishop, R.E.D., Hassan, A.Y., 1963. The lift and drag forces on a circular cylinder in a flowing fluid. Proceedings of the Royal Society Series A 277, 32–50.

Bishop, R.E.D., Hassan, A.Y., 1964. The lift and drag forces on a circular cylinder oscillating in a flowing fluid. Proceedings of the Royal Society of London A 277, 51–75.

Blevins, R.D., 1990. Flow-Induced Vibrations. Van Nostrand Reinhold, New York.

Branković, M., Bearman, P.W., 2006. Measurements of transverse forces on circular cylinders undergoing vortex-induced vibration. Journal of Fluids and Structures 22, 829–836.

de Langre, E., 2006. Frequency lock-in is caused by coupled-mode flutter. Journal of Fluids and Structures 22, 783–791.

Facchinetti, M.L., de Langre, E., Biolley, F., 2004. Coupling of structure and wake oscillators in vortex-induced vibrations. Journal of Fluids and Structures 19, 123–140.

Feng, C.C., 1968. The measurement of vortex-induced effects in flow past a stationary and oscillating circular and D-section cylinders. Master's Thesis, University of British Columbia, Vancouver.

Gharib, M.R., Leonard, A., Gharib, M., Roshko, A., 1998. The absence of lock-in and the role of mass ratio. In: Bearman, P.W., Williamson, C.H.K. (Eds.), Proceedings Conference on Bluff Body Wakes and Vortex-Induced vibrations. Washington, DC, Paper Number 24.

Goswami, I., Scanlan, R.H., Jones, N.P., 1993. Vortex-induced vibration of circular cylinders—part 2: new model. ASCE Journal of Engineering Mechanics 119, 2288–2302.

Griffin, O.M., 1980. Vortex-excited cross flow vibrations of a single cylindrical tube. ASME Journal of Pressure Vessel Technology 102, 158–166.

Griffin, O.M., Koopman, G.H., 1997. The vortex-excited lift and reaction forces on resonantly vibrating cylinders. Journal of Sound and Vibration 54, 435–448.

Griffin, O.M., Skop, R.A., Koopman, G.H., 1973. The vortex-excited resonant vibrations of circular cylinders. Journal of Sound and Vibration 31, 235–249.

Hartlen, R.T., Currie, I.G., 1970. Lift-oscillator model of vortex-induced vibration. Journal of the Engineering Mechanics 96, 577–591.

Khalak, A., Williamson, C.H.K., 1997. Investigation of the relative effects of mass and damping in vortex-induced vibration of a circular cylinder. Journal of Wind Engineering and Industrial Aerodynamics 69–71, 34–350.

Khalak, A., Williamson, C.H.K., 1999. Motions, forces and mode transitions in vortex-induced vibrations at low mass-damping. Journal of Fluids and Structures 13, 813–851.

King, R., 1977. Vortex-excited oscillations of yawed circular cylinders. ASME Journal of Fluids Engineering 99, 495–502.

Klamo, J.T., 2007. Effects of damping and Reynolds number on vortex-induced vibrations. PhD Thesis, California Institute of Technology Pasadena, California.

Krenk, S., Nielsen, S.R.K., 1999. Energy balanced double oscillator model for vortex-induced vibrations. ASCE Journal of Engineering Mechanics 125, 263–271.

Lynch, J.J., 1995. Analysis and design of systems of coupled microwave oscillators. PhD Thesis, Department of Electrical and Computer Engineering, University of California at Santa Barbara.

Maas, S.A., 1988. Nonlinear Microwave Circuits. Artech House, Boston.

McIver, D.B., 1973. Hamilton's principle for systems of changing mass. ASCE Journal of Engineering Mechanics 7, 249–261.

Mirollo, R.E., Strogatz, S.H., 1990. Synchronization of the pulse-coupled biological oscillators. SIAM Journal of Applied Mathematics 50, 1645–1662.

Moe, G., Wu, Z.J., 1990. The lift force on a cylinder vibrating in a current. ASME Journal of Offshore Mechanics and Arctic Engineering 112, 297–303.

Mureithi, N.W., Kanki, H., Nakamura, T., 2000. Bifurcation and perturbation analysis of some vortex shedding models. In: Proceedings of the 7th International Conference on Flow-Induced Vibrations, Luzern, Switzerland. Balkema, Rotterdam. pp. 61–68.

Nayfeh, A.H., 1993. Introduction to Perturbation Techniques. Wiley, New York.

Pantazopoulos, M.S., 1994. Vortex-induced vibration parameters: critical review. In: Proceedings of the 17th International Conference on Offshore Mechanics and Arctic Engineering, Osaka, Japan. pp. 199–255.

Parkinson, G., 1989. Phenomena and modeling of flow-induced vibrations of bluff bodies. Progress in Aerospace Sciences 26, 169–224.

Plaschko, P., 2000. Global chaos in flow-induced oscillations of cylinders. Journal of Fluids and Structures 14, 883–893.

Rand, R.H., Holmes, P., 1980. Bifurcation of periodic motions in two coupled van der Pol oscillators. International Journal of Non-Linear Mechanics 15, 387–399.

Sarpkaya, T., 2004. A critical review of the intrinsic nature of vortex-induced vibrations. Journal of Fluids and Structures 19, 389–447.

Simiu, E., Scanlan, R.H., 1986. Wind Effects on Structures. Wiley, New York.

Skop, R.A., 1974. On modeling vortex-excited oscillations. NRL Memorandum Report 2927.

Skop, R.A., Balasubramanian, S., 1997. A new twist on an old model for vortex-excited vibrations. Journal of Fluids and Structures 11, 395–412.

Skop, R.A., Griffin, O.M., 1973. A model for the vortex-excited resonant response of bluff cylinders. Journal of Sound and Vibration 27, 225–233.

Teufel, A., Steindl, A., Troger, H., 2006. Synchronization of two flow excited pendula. Communications in Nonlinear Science and Numerical Simulation 11, 577–594.

Vickery, B.J., Watkins, R.D., 1962. Flow-induced vibration of cylindrical structures. In: Proceedings of the First Australian Conference. University of Western Australia, pp. 213–241.

Williamson, C.H.K., Govardhan, R., 2007. A brief review of recent results in vortex-induced vibrations. Journal of Wind Engineering and Industrial Aerodynamics, doi:10.1016/j.jweia.2007.06.019.

Wirkus, S., 1999. The dynamics of two coupled van der Pol oscillators with delay coupling. PhD Thesis, Cornell University, Ithaca, NY, USA.

Wirkus, S., Rand, R., 2002. Dynamics of two coupled van der Pol oscillators with delay coupling. Nonlinear Dynamics 30, 205–221.

Woafo, P., Yamapi, R., Chabi Orou, J.B., 2005. Dynamics of a nonlinear electromechanical system with multiple functions in series. Communications in Nonlinear Science and Numerical Simulation 10, 229–251.